Supporting Information

Enhanced Sequestration of Large-sized Dissolved Organic Micropollutants in Polymeric Membranes Incorporated with Mesoporous Carbon

Wei Teng,[‡a] Nan Bai,[‡a] Jianwei Fan,[a] Dandan Li,[a] Rui Liu,[c] Jianping Yang,[a] Wei-xian Zhang,*[a] and Dongyuan Zhao*[b]

[a] State Key Laboratory for Pollution Control, College of Environmental Science and Engineering, Tongji University, Shanghai, China 200092

[b] Department of Chemistry, Shanghai Key Laboratory of Molecular Catalysis and Innovative Materials, and Advanced Materials Laboratory, Fudan University, Shanghai, China 200433

[c] Ministry of Education Key Laboratory of Advanced Civil Engineering Material, School of Materials Science and Engineering, and Institute of Advanced Study, Tongji University, Shanghai, China,201804

EXPERIMENTAL

Characterization of mesoporous carbon

Small-angle X-ray scattering (SAXS) patterns were measured with a Nanostar U small-angle X-ray scattering system (Bruker) with a Cu Kα radiation (40 kV, 35 mA). High resolution scanning electron microscopy (HRSEM) images were recorded by a Hitachi S-4800 ultrahigh resolution SEM (1 kV). Transmission electron microscopy (TEM) images were taken by a JEM 2100F microscope operated at 200 kV. Samples for TEM tests were dispersed in ethanol and then dropped onto holey carbon films. Nitrogen adsorption/desorption isotherms were measured by a Micromeritics Tristar 3020 analyzer at 77 K. Before the measurements, samples were degassed in vacuum at 180 °C for 6 h. The surface area (S_{BET}) was calculated by BET method by using the adsorption data at p/p_0 of 0.02 – 0.2. The total pore volume (V_t) was estimated from the adsorbed amount at p/p_0 of 0.995. The pore size distribution was derived from the adsorption branches of isotherms by using the BJH model.

Measurements of MC-LR and RhB

MC-LR concentration was analyzed by HPLC (LC-10AT, Shimadzu) with an ultraviolet (UV) detector (Model 2478) and a C18 column (Shim-pack VP-ODS, 4.6 x 150 mm, i.d. 5 mm). The mobile phase was a mixture of methanol-water (60 : 40) containing 0.1 % of TFA (v/v) with a 0.8 mL/min at 40°C. The detection was carried out at 238 nm with the injection volume of 50 μL.

The concentration of RhB was detected with UV-Vis spectrophotometer (Shimadzu UV-2600) at 552 nm.

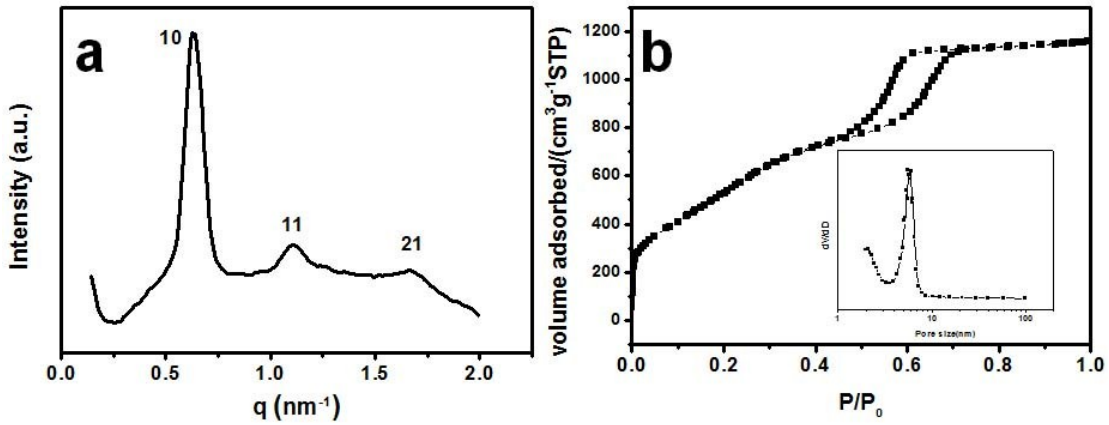

Fig. S1. SAXS patterns (a), and nitrogen sorption isotherms (b) and the corresponding pore size distribution curves (b inset) of pristine ordered mesoporous carbon.

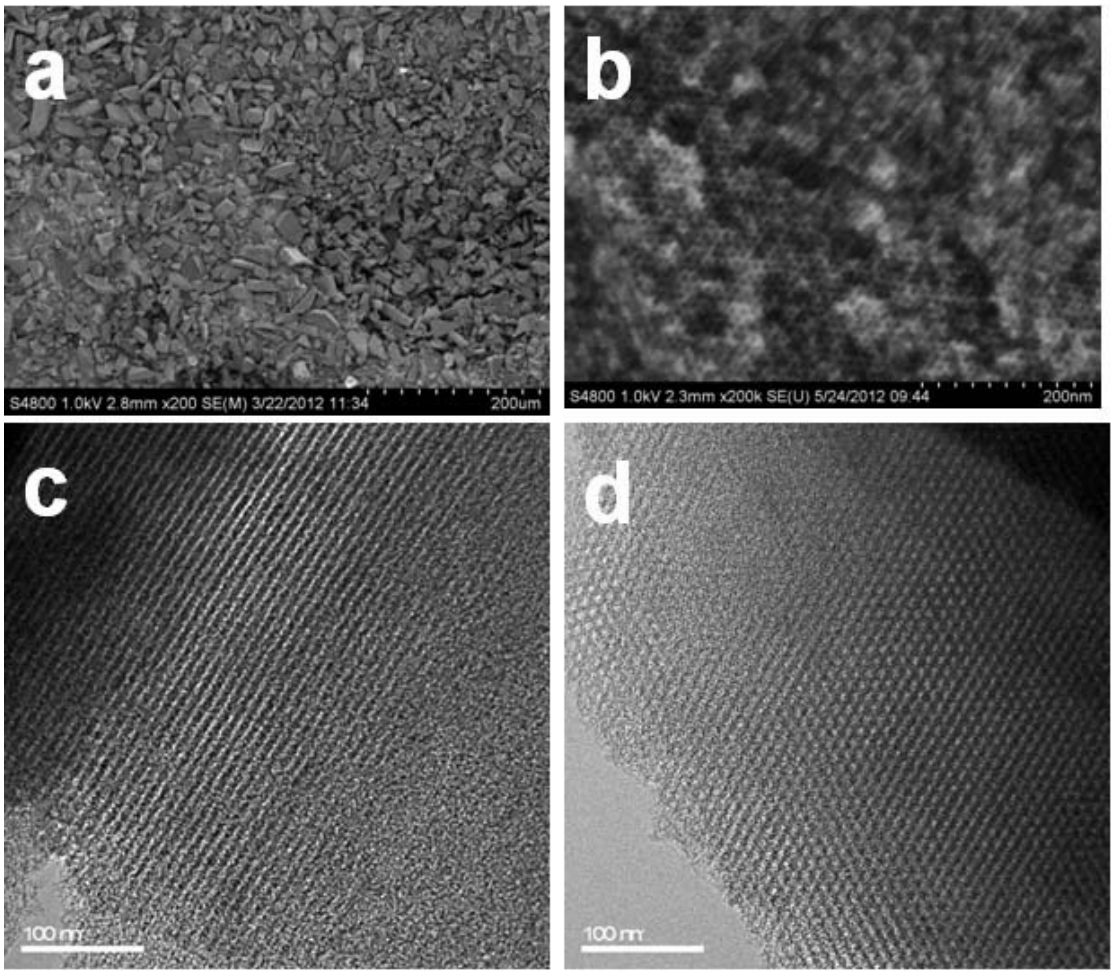

Fig. S2. SEM (a, b) and TEM (c, d) images of the pristine mesoporous carbon viewed along and perpendicular to the pore channels.

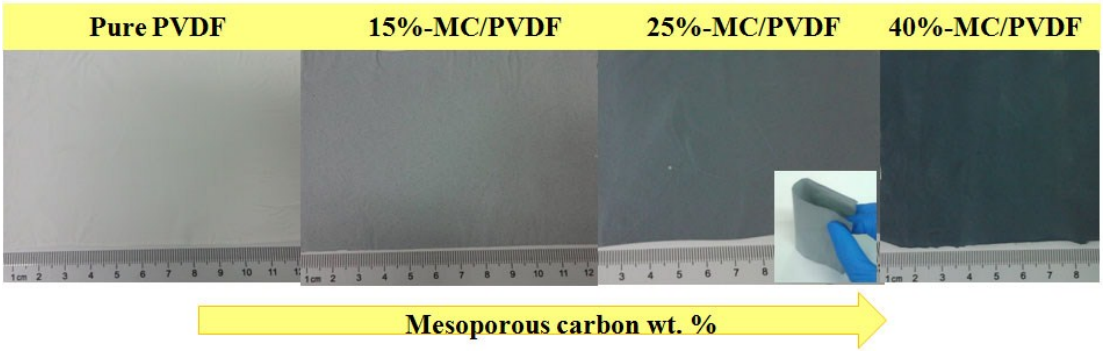

Fig. S3. Optical photographs of pure PVDF and hybrid mesoporous carbon/PVDF membranes with different carbon contents.

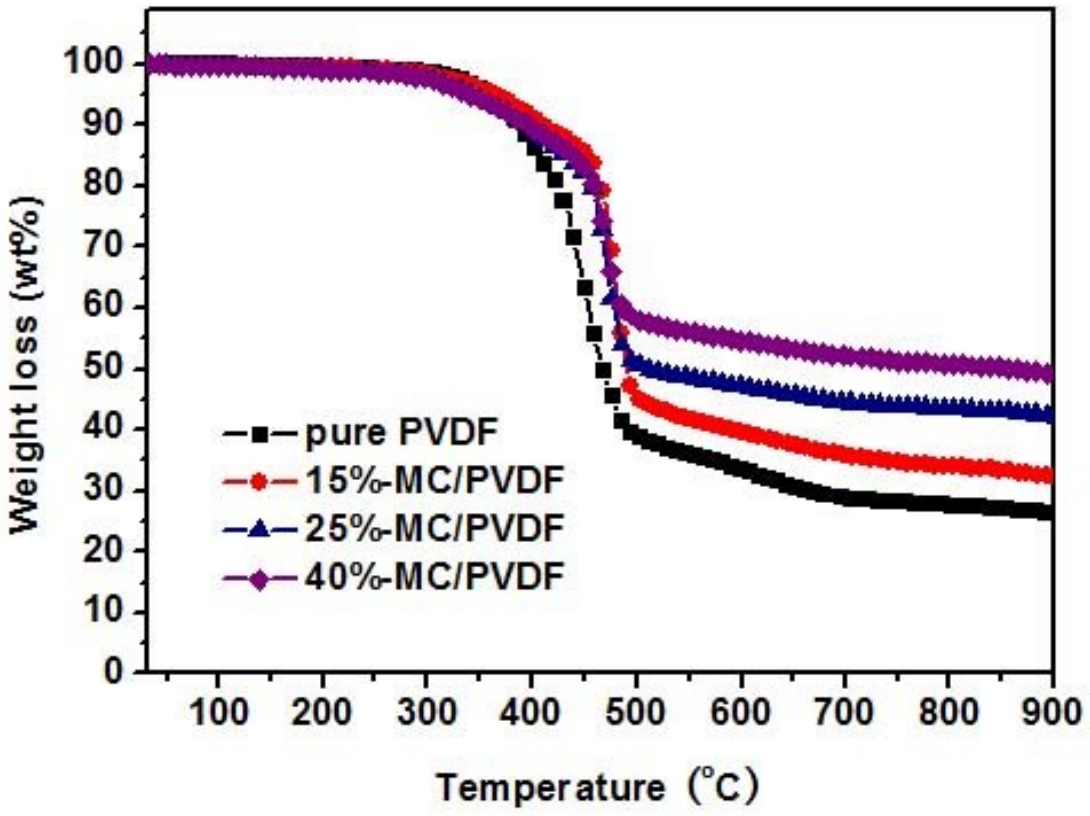

Fig. S4. TG curves (carried out in nitrogen) of pure PVDF (a) and hybrid mesoporous carbon/PVDF membranes with different carbon contents.

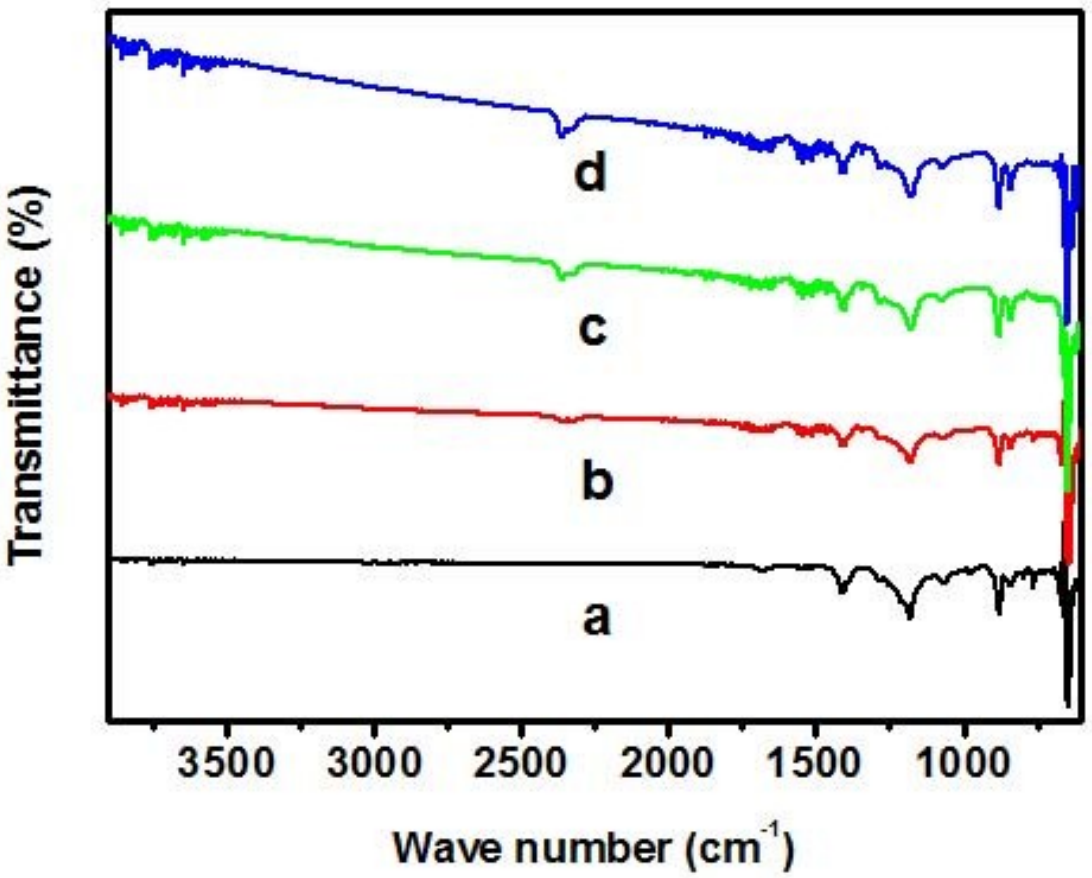

Fig. S5. FT-IR spectra of pure PVDF (a) and hybrid mesoporous carbon/PVDF membranes with different carbon contents: 15%-MC/PVDF (b), 25%-MC/PVDF (c) and 40%-MC/PVDF (d).

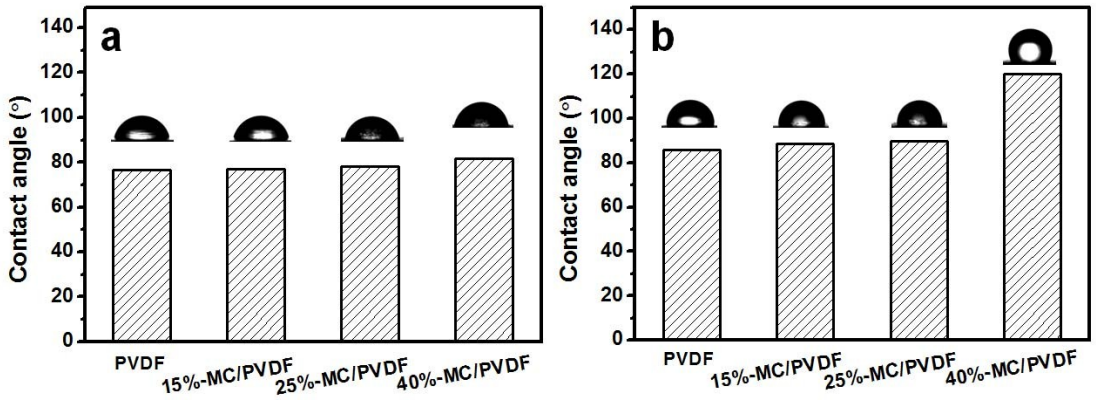

Fig. S6. Water contact angle on the top (a) and bottom (b) surface of pure PVDF and hybrid mesoporous carbon/PVDF membranes with different carbon contents. Inset is the photographs of CA measurements.

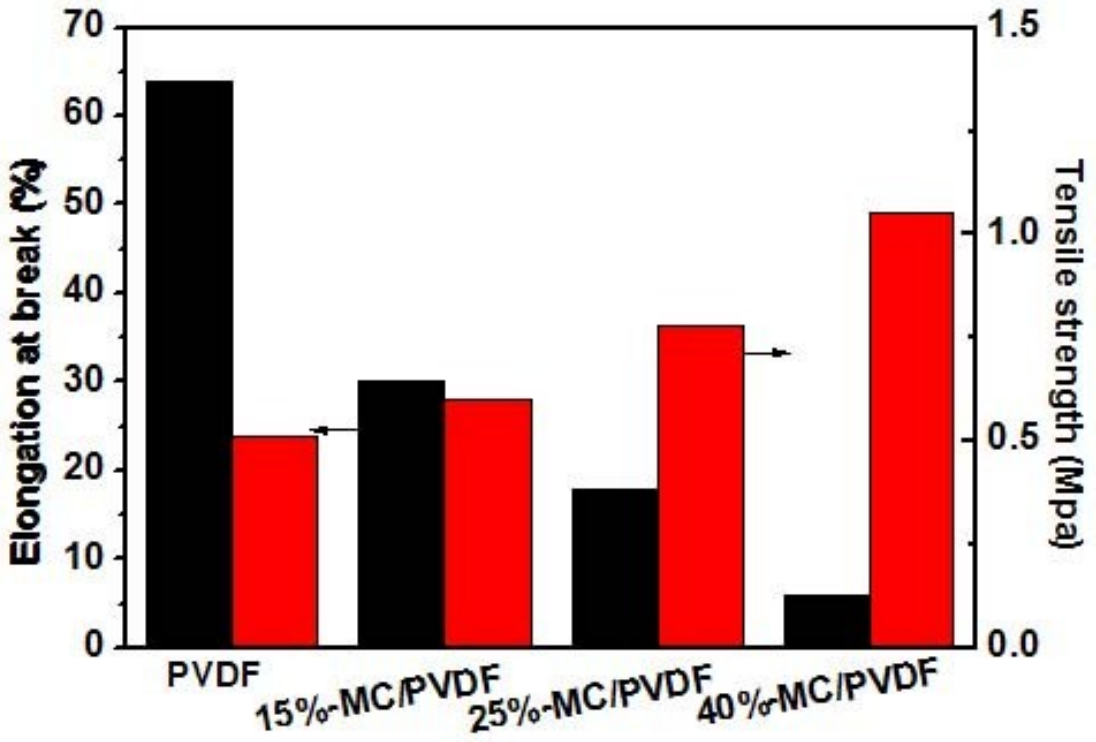

Fig. S7. Elongation-at-break and tensile strength of pure PVDF and hybrid mesoporous carbon/PVDF membranes with different carbon contents.

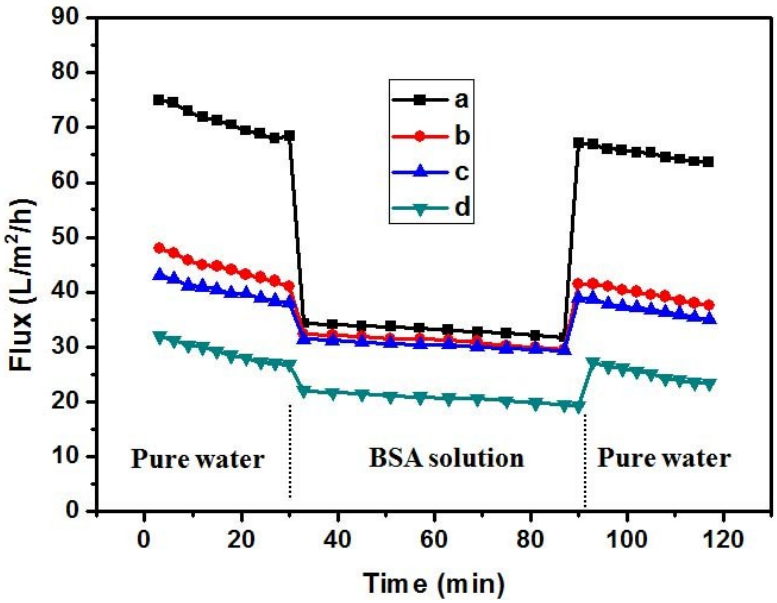

Fig. S8. Flux *versus* time of pure PVDF (a) and hybrid mesoporous carbon/PVDF membranes: 15%-MC/PVDF (b), 25%-MC/PVDF (c) and 40%-MC/PVDF (d) at 0.1 MPa with three cycles: water flux for 30 min, BSA solution flux for 60 min and water flux for 30 min again after cleaning and washing.

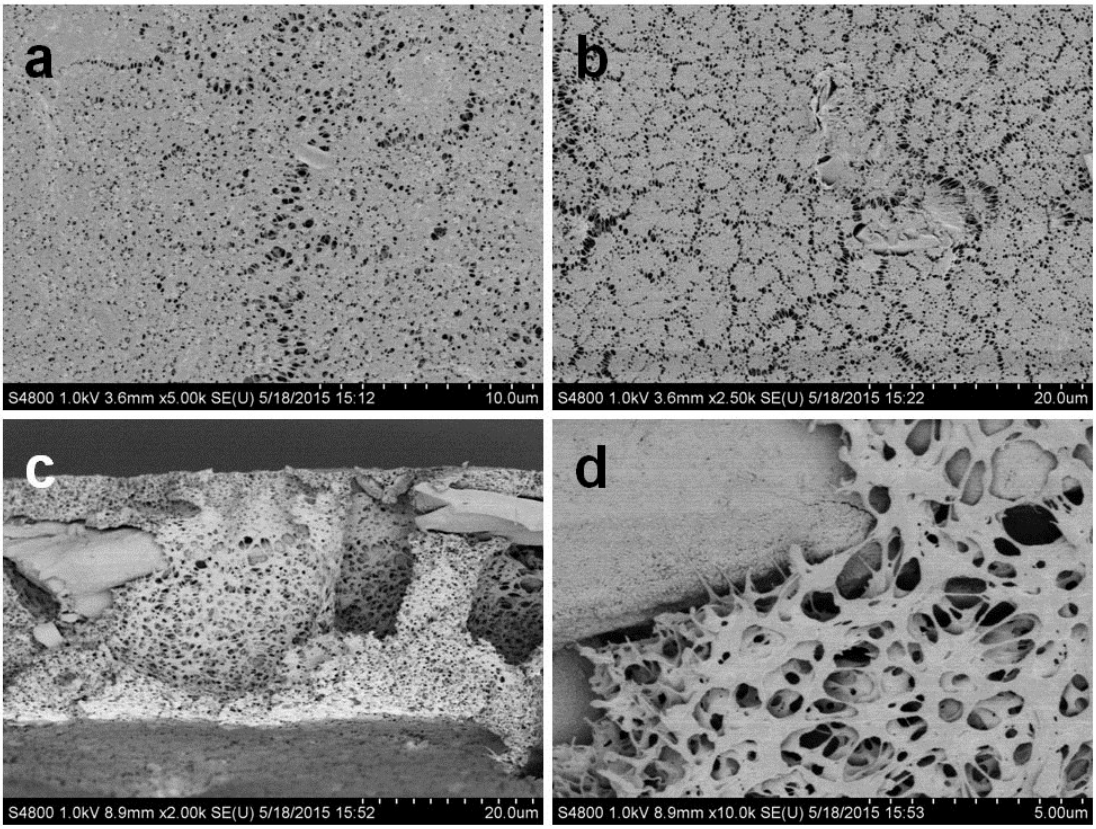

Fig. S9. SEM images of 25%-activated carbon/PVDF membrane from the top surface (a), bottom surface (b), cross-section (c) and enlarged cross-section (d) of membrane.

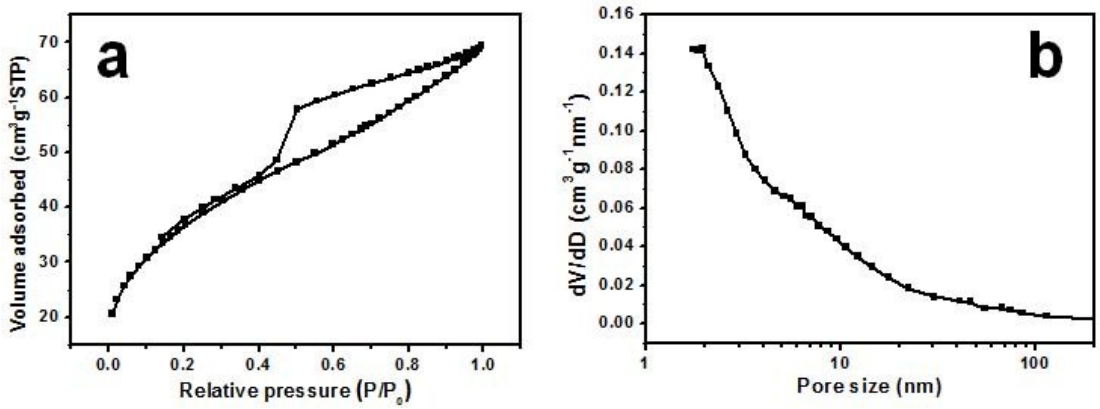

Fig. S10. Nitrogen sorption isotherms (a) and the corresponding pore size distribution curves (b) of powdery activated carbon.

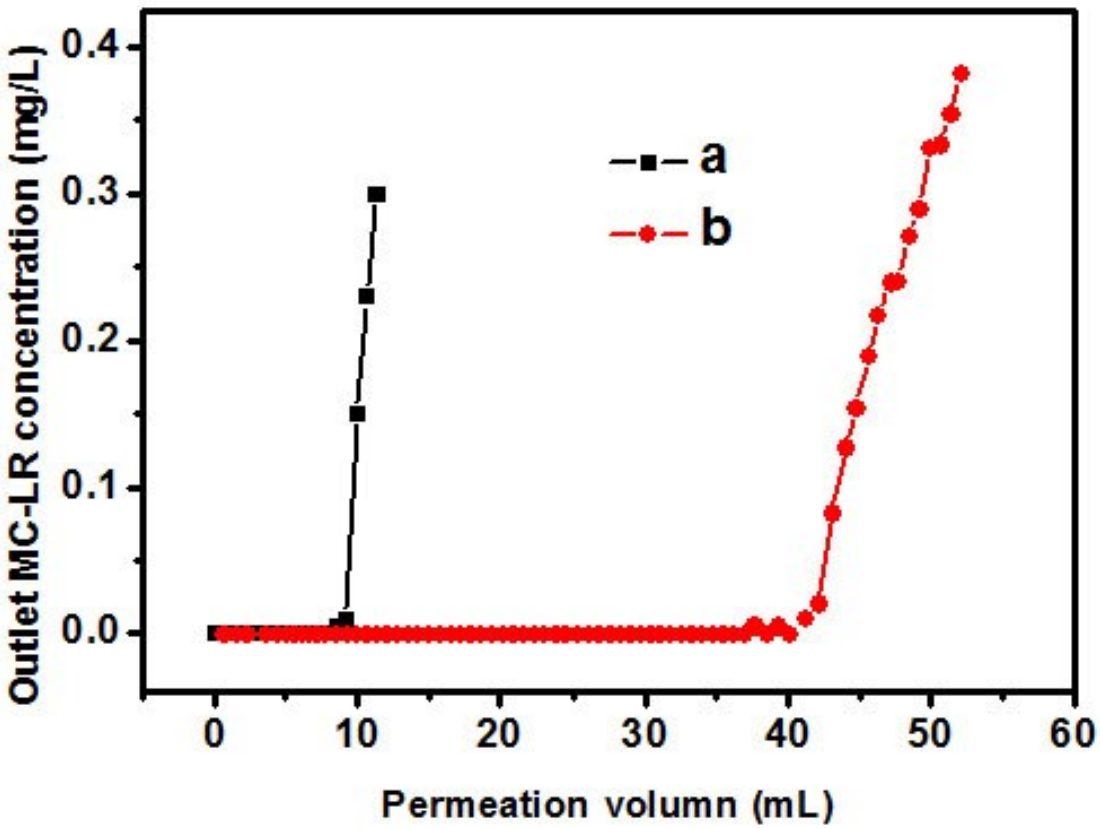

Fig. S11. Breakthrough curves of the MC-LR solutions through 25%-activated carbon/PVDF (a) and 25%-MC/PVDF (b) membrane.

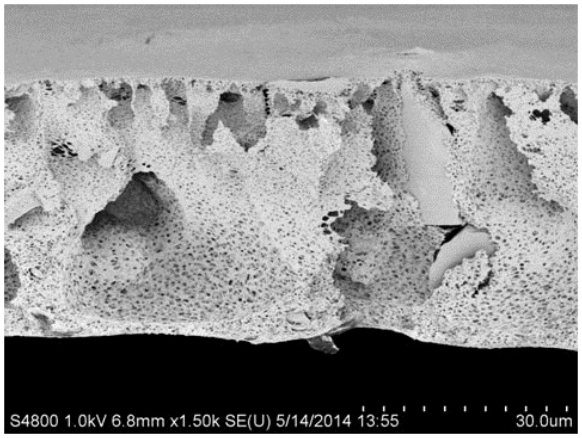

Fig. S12. Cross-section SEM image of 25%-MC/PVDF membrane after reuse.

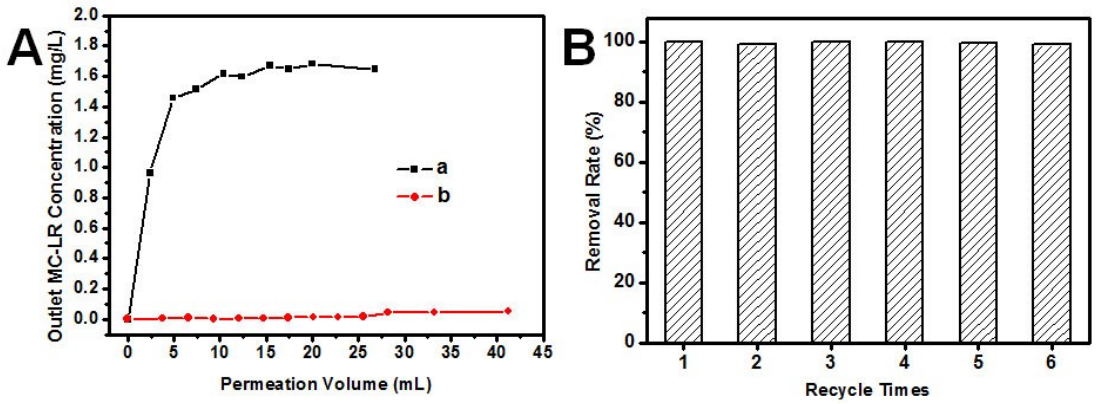

Fig. S13. (A) Breakthrough curves of the RhB solutions through pure PVDF (a), and 25%-MC/PVDF (b) membrane. (B) Removal rate of RhB for consecutive cycles through 25%-MC/PVDF membrane. All tests were conducted with a feed concentration of 2.0 mg/L , flow rate of 1.0 mL/min, at pH of 7.0.

Table S1. Structural, textural parameters and porosity of mesoporous carbon, pure and hybrid PVDF membranes with various mesoporous carbon contents.

Sample	S_{BET} (m^2g^{-1})	V_t (cm^3g^{-1})	D (nm)	Porosity (%)
MC	**1600**	**1.7**	**2.0, 5.6**	**--**
PVDF	**8**	**0.02**	**--**	**68**
15%-MC/PVDF	**178**	**0.17**	**2.0, 5.6**	**70**
25%-MC/PVDF	**400**	**0.34**	**2.0, 5.6**	**73**
40%-MC/PVDF	**550**	**0.44**	**2.0, 5.6**	**69**

Table S2. Structural, textural parameters of pristine activated carbon and hybrid activated carbon/ PVDF membrane.

Sample	S_{BET} (m^2g^{-1})	V_t (cm^3g^{-1})	D (nm)
AC	**1680**	**1.03**	**<2**
25%-AC/PVDF	**130**	**0.11**	**<2**